Computers and Electronics in Agriculture 193 (2022) 106732

Contents lists available at ScienceDirect

Computers and Electronics in Agriculture

journal homepage: www.elsevier.com/locate/compag

Detection of crop diseases using enhanced variability imagery data and convolutional neural networks

Shai Kendler [a,b,*], Ran Aharoni [a], Sierra Young [c], Hanan Sela [d], Tamar Kis-Papo [d], Tzion Fahima [d], Barak Fishbain [b]

[a] Israel Institute for Biological Research, Department of Environmental Physics, Ness-Ziona, Israel
[b] Faculty of Civil and Environmental Engineering, Technion – Israel Institute of Technology, Haifa 3200003, Israel
[c] Deptartment of Biological and Agricultural Engineering, North Carolina State University, 151 Weaver Laboratories, Campus Box 7625, Raleigh, NC 27695, USA
[d] Department of Evolutionary and Environmental Biology, University of Haifa, 199 Abba-Hushi Avenue, Mt. Carmel, 3498838 Haifa, Israel

ARTICLE INFO

Keywords:
Crop disease
Convolutional Neural Networks
Classification
Precision agriculture
Generalization

ABSTRACT

The timely detection of crop diseases is critical for securing crop productivity, lowering production costs, and minimizing agrochemical use. This study presents a crop disease identification method that is based on Convolutional Neural Networks (CNN) trained on images taken with consumer-grade cameras. Specifically, this study addresses the early detection of wheat yellow rust, stem rust, powdery mildew, potato late blight, and wild barley net blotch. To facilitate this, pictures were taken in situ without modifying the scene, the background, or controlling the illumination. Each image was then split into several patches, thus retaining the original spatial resolution of the image while allowing for data variability. The resulting dataset was highly diverse since the disease manifestation, imaging geometry, and illumination varied from patch to patch. This diverse dataset was used to train various CNN architectures to find the best match. The resulting classification accuracy was 95.4 ± 0.4%. These promising results lay the groundwork for autonomous early detection of plant diseases. Guidelines for implementing this approach in realistic conditions are also discussed.

1. Introduction

Crop diseases such as Yellow Rust (YR), Powdery Mildew (PM), Late Blight (LB), Net Blotch (NB), septoria and others pose a threat to crop production worldwide. This scourge is often exacerbated when disease pathogens mutate and spread to new and unexpected locations. For example, the world global yield loss due to wheat pests is estimated to be 21.5% (Savary et al., 2019). Since YR spreads very fast, with a latency period of two weeks, it is ranked fourth in terms of global yield loss (2% globally and represents about 5% of all losses in China and Western Europe (Savary et al., 2019)). Murray et al. (1994) reported that between 1984 and 1987, Stripe (yellow) rust caused a wheat yield loss of up to 84% in southern New South Wales, Australia. PM causes a 1% global yield loss in wheat (1% globally with 2.5% in Europe and 3.25% in China (Savary et al., 2019)). Stem rust in wheat is a major concern in East Africa, causing a yield loss of 9%, which can even increase to a total yield loss of 50% in susceptible cultivars (Soko et al., 2018). NB is one of the most devastating diseases affecting barely. It can cause a loss of up to 44% in specific regions (Jayasena et al., 2007). In Israel, the emergence of NB in the mid-1950s caused a shift in the major cereal crop from barley to wheat (Kenneth, 1960). LB affects potatoes, causing a 6% yield loss globally (Savary et al., 2019).

Resistance genes have been used to mitigate the losses caused by these diseases (Adhikari et al., 2020; Akino et al., 2014; Hafeez et al., 2021; Vanderplank, 2012; McIntosh et al., 2013). However, resistance often declines rapidly as the diseases mutate and spread to new and unexpected geographic regions. Hence, agrochemicals, such as fungicides, pesticides, and insecticides, are still essential in modern agriculture. While mitigating the disease, agrochemicals can harm the environment and impose an additional economic burden. This points to the need for an integrated pathogen management strategy that combines disease detection and an optimal agrochemical application. The first step towards this optimization is to treat the disease at its early stages before it spreads to large areas, so agrochemical use is restricted to locations where they are needed. Unfortunately, few farmers apply this type of approach, and the usage of agrochemicals still depends on their knowledge and cooperation (Giomi et al., 2018). This underscores the need for reliable, accessible, automatic crop monitoring technologies.

* Corresponding author.
E-mail address: skendler@technion.ac.il (S. Kendler).

https://doi.org/10.1016/j.compag.2022.106732
Received 24 May 2021; Received in revised form 17 November 2021; Accepted 17 January 2022
Available online 21 January 2022

Crop diseases can be detected by biochemical testing of the plants, inspection by experts, and remote sensing followed by automated data analysis. Biochemical tests are accurate but are expensive and slow (Sankaran et al., 2010). Experts' examination provides high reliability, if available, but only covers relatively small areas. Remote sensing, utilizing sensors mounted on satellites and aerial platforms, provides a solution since they can cover large areas (Atzberger, 2013; Chan and Paelinckx, 2008). To this end, both hyperspectral (Dhau et al., 2018) and multispectral (Yuan et al., 2017) imagers have been used for airborne spectral analyses in precision agriculture. The spatial resolution of such systems may suffice for plant growth and coverage estimation (Duveiller and Defourny, 2010) but fall short when it comes to detecting subtle changes in the field that can occur at the centimeter scale (such as textural or color changes in infected leaves) during the early stages of crop diseases (Aharoni et al., 2021). Furthermore, during these early stages, the size of the infected area in the field, might be smaller than a single pixel in the image, even for a high-resolution sensor (Houborg et al., 2015).

Textural information may compensate for the reduction in spectral resolution of aerial imagery. Sub-millimeter textural information can be obtained by imaging from a short distance using commercially available RGB cameras. By fusing these spectral and spatial data, highly accurate classifications can be achieved. For example, Ferentinos identified 58 diseases in 25 different plants using a convolutional neural network (CNN) trained on RGB images (Ferentinos, 2018). The images were obtained in laboratory conditions, i.e., with controlled illumination and background. Ferentinos used a freely available dataset (PlantVillage) comprising nearly 90,000 images of healthy and unhealthy plant leaves (Hughes and Salathe, 2015). The classification accuracy exceeded 99% for the PlantVillage dataset. The high accuracy obtained using CNNs is attributed to their flexibility to exploit non-linear association between features extracted from the image and the prevalence of the disease. Simpler models that assume linearity between these two phenomena apply strong assumptions on the problem, which often do not hold in reality. The strength of CNN is that the functional relationship between the two observed phenomena, i.e., image features and the presence of the disease, maybe of any nature and is captured by the CNN approach; therefore, there is no need to limit the possible connection to a linear relationship. The main limitation of CNNs is that they require large data sets for training. Hence, linear classification models are still attractive. For example, Shin and Balasingham compared hand-craft feature-based support vector machine (SVM) and CNN for automatic polyp classification during colonoscopy. Image features were extracted using a histogram of oriented gradient (HOG) and then classified using SVM. The resulting classification accuracy using the HOG/SVM method was 81.7%. In order to improve the accuracy, the hue histogram features were combined with the HOG features resulting in 84.2% accuracy. For comparison, using the same dataset, the CNN classification accuracy was 92.7 without the need for hand-crafting the features (Shin and Balasingham, 2017). Similar results were reported in the case of target recognition in infrared images. Visual features were hand-crafted using the strongest 80% features computed using Speeded-up Robust Feature Transform (SURF) and then classified using SVM resulting in classification accuracy of 90.8% compared to 97.9 with CNN (Yardimci and Ayyıldız, 2018).

Boulent et al. surveyed 19 crop disease classification studies that implemented CNNs and found disease classification accuracies above 90%. They pointed out that classification could be very accurate when the data are obtained in a highly controlled environment using even illumination, uniform background, and imaging geometry, as in 13 out of 19 studies surveyed. A more challenging situation is when the target is well focused and occupies a large portion of the image, but background and illumination are uncontrolled. The most challenging situation is when the image acquisition process is not optimized for a specific area or phenomenon. The first approach results in superior classification accuracy but performs poorly on data from different sources (Boulent et al., 2019). To this end, Mohanty et al. trained a CNN classification model using the PlantVillage database and obtained 99.35% accuracy. However, the CNN classification accuracy dropped below 32% when the test was repeated on images downloaded from the internet that pertained to a different domain (Mohanty et al., 2016). Hence, high classification accuracy does not guarantee generalizability (Feng et al., 2019; Zheng et al., 2018).

The main reason for the poor generalization of CNNs is the large number of parameters incorporated into the optimization of the CNN models compared to the number of samples, which may result in overfitting. Generalization can be improved by using regularization techniques such as L1-, L2-norms and dropouts that reduce the CNN optimization to a simple solution with fewer parameters and a lower likelihood of overfitting (Feng et al., 2019). Zheng et al. developed a two-stage algorithm, where the first stage detects anomalies, and the CNN is retrained in the second stage using the anomaly detection results to regularize the feature boundaries by utilizing a loss function for outliers (Zheng et al., 2018).

Diseases appear in many different ways in the image and are immersed in irrelevant information, making its accurate classification challenging. Recently, several attempts to deal with the large diversity of crop disease manifestation have been reported. A two-step approach for diseases classification was recently presented; in the first stage, the image is segmented to isolate suspected regions which are then classified using a CNN. This two-step approach significantly has increased the accuracy compared to a single-stage approach resulting in 94% classification accuracy for ten diseases for a data set comprised of images taken in a controlled environment (60%) and uncontrolled environment (40%) (Arnal Barbedo, 2019). Tassis et al. have developed a three-step classification method, based on instance and semantic segmentation, to identify diseases and pests in coffee leaves. An R-CNN network is used for instance-segmentation followed by a semantic segmentation, using UNet and PSPNet networks. At the third stage, the image is classified using ResNet (Tassis et al., 2021). This three-step classification process of a single disease results in a classification accuracy of 94.25%. Sharma et al. have used segmented images to train CNN models for plant diseases classification. The classification accuracy for ten different diseases in tomatoes was 98.6% for the segmented dataset that focused on the phenomena of interest. Furthermore, the confidence for correct classification was considerably increased by image segmentation (Sharma et al., 2020).

This paper describes a new approach that responds to the need to effectively incorporate variability into training data by dividing each image into several patches - *multipatch*. In this fashion, the same phenomenon is sampled under different conditions, such as illumination intensity, focus quality, relative geometry, in the various patches. The multipatch approach, presented here, increases the amount of data presented to the CNN and retains the original images' spatial resolution, thus providing more information to the CNN. The information gained by splitting each image into several patches results in a more variable dataset used to train the CNN, thus having a better chance to deal with realistic situations which are highly diverse. As a result of its improved generalizability, CNNs, trained using this method, have an improved generalization capability; thus, they can handle data from different sources collected on-site without modifying the scene, background, or illumination.

2. Methodology

2.1. Expanding data variability

When imaging a diseased crop at millimeter resolution, signs of the disease may be manifested in several locations in the image as a function of disease severity. Fig. 1 shows an example of wheat infected with powdery mildew (PM), which appears as white or light brown spots in several places in the image. Note that different parts of the plant are

Fig. 1. An image of wheat leaves infected with powdery mildew (PM). The infection is manifested by white light- brown spots. Some of these spots are marked with ellipsoids. It shows that in some locations the image is well focused (red ellipsoids) but in others is more poorly focused (black ellipsoids). Similarly, the illumination is uneven, as shown by the two adjacent arrows indicating the bright area (yellow arrow) and the dark area (gray arrow).

imaged at different angles and distances. Hence, some parts of the image are well focused, and others are not; similarly, the illumination intensity is not uniform.

Modern cellphones take high-resolution images that can be split into several patches. Thus, each patch captures a specific manifestation of the crop disease and imaging conditions, providing a highly variable set of images that should result in a robust CNN for crop disease identification. The multipatch method also obviates the need to downsample the image (typically to ~ 224X224 pixels) and essentially degrades its resolution. Thus, fine details in the image are retained and potentially can improve classification as demonstrated for glioma and non-small-cell lung carcinoma (Hou et al., 2015). Fig. 2 shows an example of the effect of such downsizing. It shows that while coarse details remain after the image has been downsized, finer details are lost. Hence, one can expect that trying to detect these details after downsizing will be difficult.

Note that crop disease might only be manifested in a few patches out of the entire image in its early stages. Thus, a decision-making policy must be defined to analyze the CNN results that stipulate the number of positive indications required to consider the entire plot to be infected.

At first, this process may appear to resemble the data-augmentation technique, which is ubiquitous in deep-learning applications (Shorten and Khoshgoftaar, 2019), including precision agriculture to cope with real-life situations in which data is limited (Hedayati et al., 2019). However, data-augmentation techniques involve several digital transformations such as scaling, rotation, noise injection, and translation. The underlying assumption is that the test set diversity can be explicitly predicted and digitally simulated in the training set. The multipatch method works around this assumption and increases the dataset diversity by dividing high-resolution images into small patches that the CNN can process.

Other methods to increase the dataset variability to improve CNN generalization capabilities have been reported. For example, Wang et al. collected a large and highly diverse dataset comprising of 49,700 images. Agriculture experts manually annotated 264,700 bounding boxes for locating pests in various conditions (Wang et al., 2021). An alternative approach to increasing the dataset diversity is to increase the CNN robustness towards domain changes using the domain-adversarial neural network – DANN (Ganin et al., 2017). The network is trained to accurately predict the labeled data in the source domain using features that are invariant to domain changes in the target domain. Elshamli et al. showed that crop detection using DANN outperforms traditional methods (Elshamli et al., 2017). Wu et al. showed that detecting oil trees using DANN is 9.04%-15.30% more accurate than other domain adaptation methods (Wu et al., 2020).

The multipatch approach, i.e., splitting the image into several patches, is a simple technique to increase dataset diversity using a relatively small dataset. It does not use physical modeling or artificial data augmentation, or any other assumption on the data. The resulting dataset is highly diverse since the disease manifestation, imaging geometry, and illumination variations are retained and not degraded by image downsizing before presenting it to the CNN. The annotation procedure is simple; one must ensure that the phenomena of interest

Fig. 2. Images of a wheat field. Left- original (4000x6000) image, right - downsized image to 224X224 pixels, typical of CNNs. The general view is similar, but the lower spatial resolution is obvious.

appear in the entire image. Once this is accomplished, the same label can be used for all patches.

2.2. Materials and methods

Images of wheat plants infected with PM were taken after inoculation of the wheat, according to the following protocol. Two near-isogenic lines (NILs) of bread wheat (Triticum aestivum), one with the Powdery Mildew resistance gene PmG3m (ZZPmR), and one susceptible to PM (ZZPmS), were inoculated with the highly virulent Bgt isolate #70. All plants were germinated simultaneously to avoid any bias due to plant age. About 500 plants were inoculated 15, 12, 10, and 5 days before the images were taken at 28 days after germination. A control experiment was conducted using susceptible and resistant lines (ZZPmR and ZZPmS) with no inoculation.

Images of wheat infected with yellow rust (YR) were obtained from a freely available collection: the CGIAR, Computer Vision for Crop Disease (Hussain, 2020). The experiments with YR were conducted in Bet-Dagan, Central Israel, during the 2017–2018 cropping seasons where YR was artificially inoculated. Images of wheat infected with stem rust (SR) were also obtained from the CGIAR collection. Images of the healthy wheat plants were obtained from all the above sources. Images of both healthy wild barley (Hordeum spontaneum) and plants infected with net blotch (NB) were obtained in a wild field near Kiryat Tivon, in northern Israel. Both healthy and infected potato images with late blight (LB) were taken in the central part of the Israeli Negev.

Most photos were taken using commercially available cellphones (such as Oneplus 6, Redme, and others); the remainder (about 10% of the PM images) were taken using a Nikon D850 with a Nikon 24–70f/2.8 lens. Images using the cellphone were taken in the automatic mode, whereas photos taken with the DSLR camera were taken at f/8, focal length 28 mm, shutter speed 1/320 s, and auto iso (auto gain). All images were labeled by an agriculture expert who is familiar with these diseases. The labels used for this study are listed in Table 1.

The dataset was then randomly split into training, validation, and test sets (64%, 16%, and 20%, respectively). The images were divided into 36 patches. In the case of potato plants, late blight is manifested in the center of the image. Thus, only the nine patches located in the center of the image were used. In all the other crops, uninformative patches containing sky, soil, and other irrelevant objects were manually removed from the dataset. Each patch was labeled according to the original image label. The number of patches pertaining to each label in the dataset appears in Table 1. Fig. 3 presents a few images of each label.

Using the same CNN architecture, the multipatch method is compared against full image analysis, i.e., processing the entire image without splitting the images into patches. In most cases, the disease is manifested all over the image, resulting in a fairly convenient situation for the whole image approach. A more complicated situation occurs when the CNN is faced with an image that the disease is manifested in a small portion of the image. For that purpose, an additional date set of wild barley (Hordeum spontaneum) was used. These images were taken at the early stages of infection with net blotch. In this set, the infection is manifested in only a fraction of the entire image. In most cases, only 2–3 lesions were observed in the entire image, typical of fungal diseases that start with small foci and spread unevenly.

Table 1
List of plants, conditions, labels, and the total number of patches in the dataset.

Plant	Condition	Label	number of patches
Wheat	PM	D_PM	9160
	SR	D_SR	4650
	YR	D_YR	5820
	Healthy	H	14,430
Potato	Healthy	Po_H	2980
	LB	Po_LB	920
Wild barley	Healthy	WB_H	4250
	NB	WB_NB	11,250

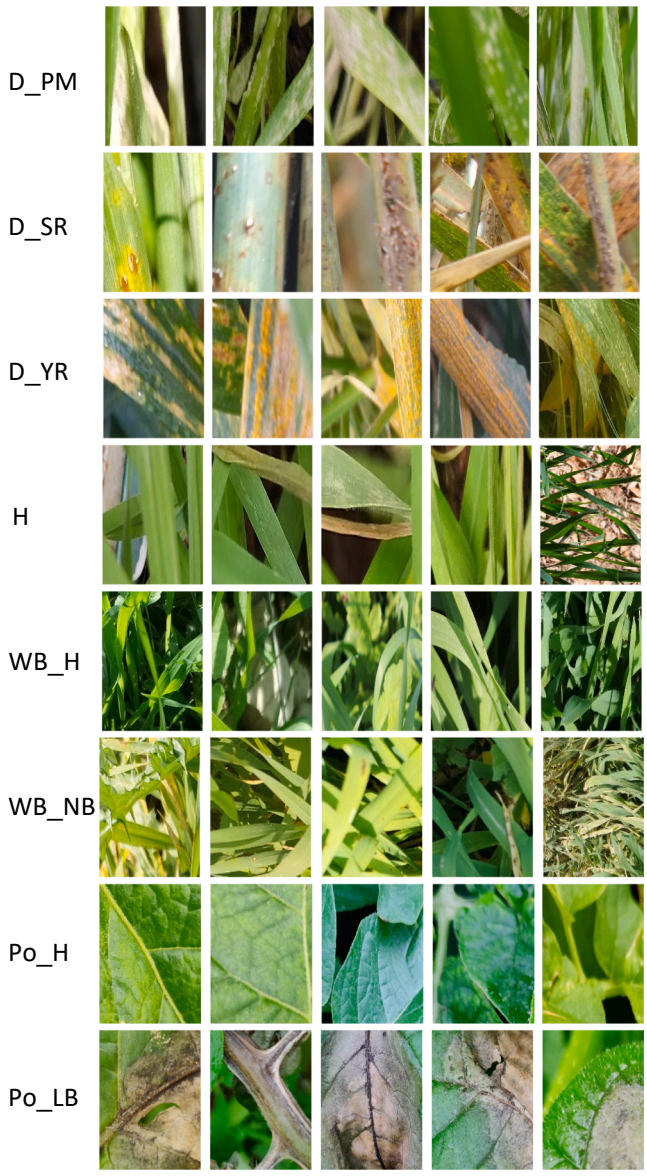

Fig. 3. A few examples of patches associated with different labels (see Table 1 for the labels).

2.3. CNN classification model calculation and testing

Several well-established CNN network architectures were used for the classification process: AlexNet (Krizhevsky et al., 2012), Inception v3 (Xiaoling Xia et al., 2017), GoogleNet (Ballester and Araujo, 2016), ResNet50 (Mukti and Biswas, 2019; Saleem et al., 2019), and ResNet101 (Saleem et al., 2019). A transfer learning strategy was applied to refine the network parameters and adapt them to the problem at hand (Pan and Yang, 2010). Table 2 lists nine sets of hyperparameters that were used during the multipatch method evaluation. These hyperparameter sets were also used to compare the performance of the multipatch with the whole image approcach.

The hyperparameters sets performance are compared using the networks' classification accuracy, which is defined as:

$$Accuracy = \frac{Number\ \ of\ \ correct\ \ predictions}{Total\ \ number\ \ of\ \ predictions} \quad (1)$$

A false-negative (FN) event was said to occur when the CNN model

Table 2
List of transfer learning hyperparameter sets used for the multipatch method development and comparison to the classical method that uses the full image.

	Hyperparameter set								
Property	Set 1	Set 2	Set 3	Set 4	Set 5	Set 6	Set 7	Set 8	Set 9
solver	Stochastic Gradient Descent with Momentum (Qian, 1999)								
Initial learning rate	0.0015				0.01	0.003			0.01
Learning rate schedule	piecewise								
Learning rate drop factor	0.5	0.5	0.5	0.5	0.2	0.2	0.2	0.2	0.2
Learning rate drop period	2				5				
L2 regularization	0.005	0.05	0.005	0.05	0.05		0.005	0.0001	
Max Epoch	30								
MiniBatch size	32	32	64						

incorrectly labeled an image of diseased plants as healthy, regardless of the actual disease displayed in the image. A false-positive (FP) event was defined as the case where the CNN model incorrectly labeled an image as diseased, irrespective of the disease type. The uncertainty in the accuracy calculation is estimated by a k-fold cross-validation process ($k = 5$) and taking the standard deviation.

3. Results

3.1. Hyperparameter tuning

Table 3 lists the accuracy obtained in the multipatch method with the GoogleNet, ResNet 101, and InceptionResNetv2. The latter is a large CNN, and therefore, only a few computations are reported.

The accuracy obtained with the ResNet 101 CNN is, in most cases, the highest, for seven out of the nine hyperparameter sets, the accuracy is above 90% and above 95% for four sets with an uncertainty of $\pm$ 0.4%. The accuracy obtained with the GoogleNnet is lower in all cases and failed to converge for hyperparameter set #5. The InceptionResNetv2 performed similarly to the ResNet 101 CNN and was not used for further computations. Sets #3, #4, and #7 were also used to evaluate other CNNs and compare them to the classical method that uses the entire image for training and testing.

3.2. Method evaluation

Fig. 4 presents the classification results obtained with sets Sets #3, #4, and #7 with the multipatch method compared to the whole image approach. It shows that the multipatch method provides, in most cases, accuracies higher than 90%. Using AlexNet and GoogleNet CNN combined with hyperparameter set #7 reduces the accuracy below 90%. With CNN ResNet 101 accuracy of 95.4 $\pm$ 0.4% is achievable.

Compared to the whole image analysis, the accuracy obtained with the multipatch method is higher and more consistent over different CNN architectures and hyperparameter sets. Note that this comparison was performed using images in which the disease is manifested over the entire image. In a more challenging comparison, a trained CNN (ResNet101, set #3, trained and tested using the whole image) was challenged with a date set of wild barley (*Hordeum spontaneum*) images at the early stages of infection with a net blotch in which only 2–3 lesions were observed in the entire image. Our efforts to classify the entire image at this stage of the disease resulted in a high false-negative rate. In comparison, the multipatch method succeeded in identifying the diseased patches demonstrating the robustness of the multipatch trained CNN.

In Fig. 5, the classification results, obtained with the multipatch method, are depicted in the form of a confusion matrix (using ResNet101, set # 3) that compares the true class (y-axis) to the class predicted by the CNN (x-axis). The diagonal terms represent the number of accurately classified patches, and the off-diagonal represents incorrect classifications. The chart is accompanied by a row-normalized summary and a column-normalized summary. The vertical row-normalized summary represents the true-positive and false-positive rates (representing the class-wise recalls, i.e., the percentages of correctly/incorrectly classified observations for each true class). The horizontal column-normalized summary represents the positive predictive values (representing the class-wise precisions, i.e., the percentages of correctly and incorrectly classified observations for each predicted class).

Note that out of the total patches classified as healthy (H), 4.6% were diseased, in most cases due to infection by PM or YR. Since this classification was made at the single patch level, the patches making up the frame classification results could be examined before making the final decision. This examination relied on the occurrence of a certain class in an image. It seems reasonable to assume that as the number of patches in the same image that belong to the same class increases, this classification's validity should also increase. To test this hypothesis, the probability distribution of obtaining repeated true or false patch classifications from a single image was calculated. The analysis showed that correct identification occurred in most cases; for example, in images of healthy wheat, the maximum number of wrongly identified patches (false positive) was five, whereas true negatives occurred in most patches. A similar difference in the probability distribution was found for other cases studied here. These differences can be used to further improve this method by setting a static or adaptive threshold value for the number of patches from the same image that belongs to a specific class to classify the entire image.

4. Discussion and conclusion

This study illustrates the advantages of using consumer-grade RGB cameras to identify crop diseases from a short distance, typically 0.75–0.3 m. The images were cropped into separate patches and then utilized to train and test a CNN using various popular network architectures. Note that the training was performed on a uniform set of images; in other words, all the patches belonged to the same label. The resulting classification accuracy for the test set was 95.4 $\pm$ 0.4% using the ResNet 101 CNN, with other CNNs architectures providing similar

Table 3
The accuracy obtained in the multipatch method for different sets of hyperparameters.

	Hyperparameter set								
CNN	Set 1	Set 2	Set 3	Set 4	Set 5	Set 6	Set 7	Set 8	Set 9
GoogleNet	94	77.1	92.9	85.1	–	76	93.7	94.1	94
ResNet101	95.4	91.1	95.4	94.8	73.6	81.7	95.4	95.3	93.6
InceptionResNetv2	94.9	94.2							

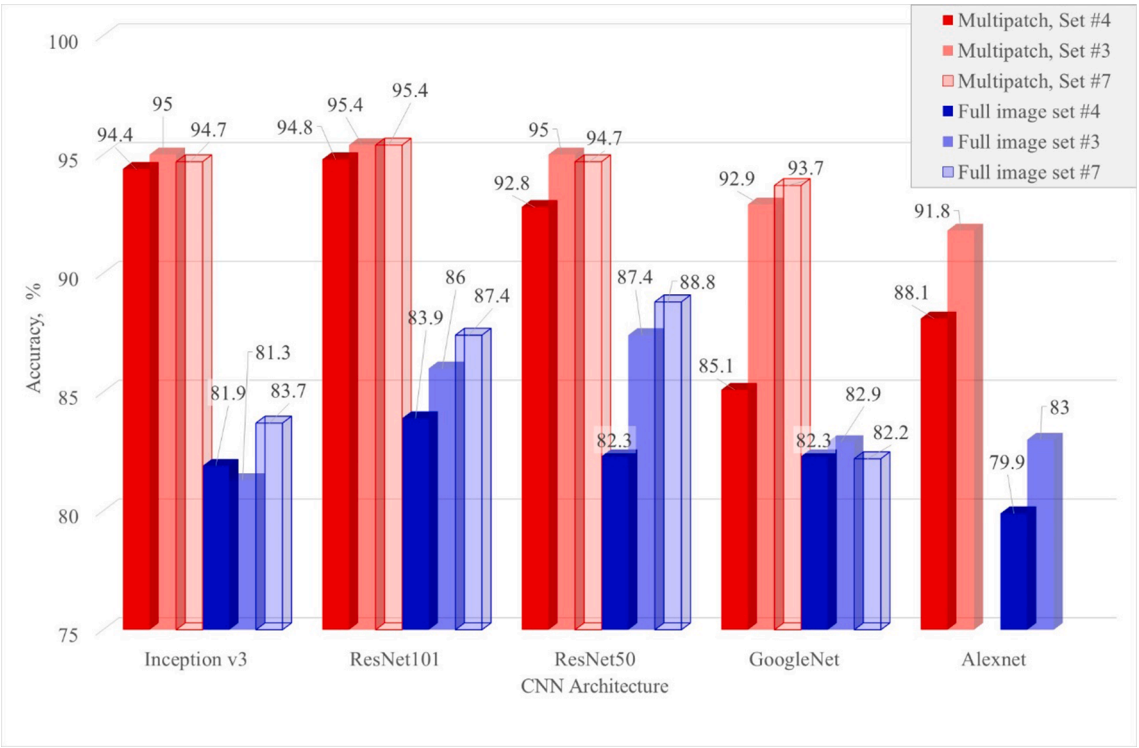

Fig. 4. Classification accuracies obtained with different CNNs and hyperparameters sets 3, 4, and 7. Results obtained with the multipatch method are in red shades bars compared to the classical method in blue shade bars (see graph legend).

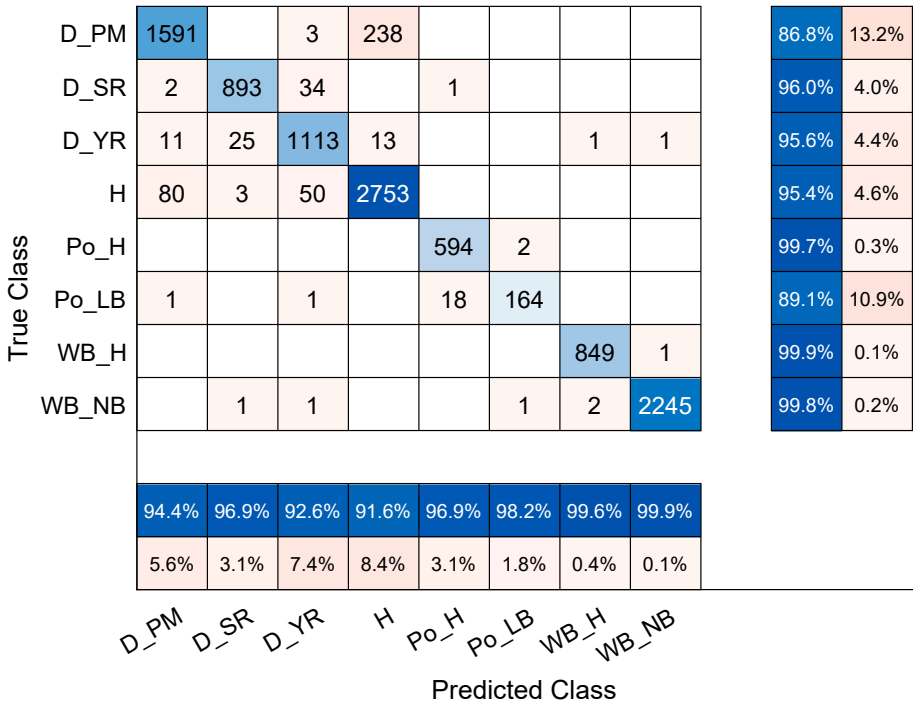

Fig. 5. The confusion matrix obtained when classifying diseased and healthy wheat (D), wild barley (WB), and potatoes (Po) using the CNN ResNet 101 (set 3). See Table 1 for the labels.

results. Both the train and test images were taken in the field without modifying the background, illumination, or manipulating the scene. A similar level of crop disease classification accuracy and even higher have been reported using images taken in controlled situations (Ferentinos, 2018; Hughes and Salathe, 2015). This finding is not surprising, as Boulent et al. pointed out that controlling the imaging (illumination, sensor object distance, angle, background) improves classification accuracy but decreases generalizability (Boulent et al., 2019). Indeed, it has been shown that CNN trained and tested with images obtained at controlled conditions can achieve 99.35% classification accuracy for

these images but less than 32% for data obtained under uncontrolled conditions, e.g., illumination, sensor-to-object geometry (Mohanty et al., 2016). The manifestation of the disease was the same regardless of the imaging procedure. However, the number of possible variations in a real-life situation remains considerable. Even in the same image, the light intensity and focus quality can change dramatically. When following the standard procedure and using the entire image for training, the algorithm processes an averaged dataset that smooths these variations. Additionally, if the disease manifestation is localized, its effect on the entire image can be small. Valuable information is also lost when downscaling the images to reduce CNN computational complexity. By contrast, splitting the images into several patches retains the fine details and preserves the variability, resulting in a highly diverse training set leading to a robust CNN. This splitting can be harnessed to account for situations in which the disease manifestations are restricted to a small portion of the image, typical of the early stages of several crop diseases. The capability of the multipatch method to handle such situations is a result of an improved generalization capability that is also reported in this study.

Recently, multiple-step CNNs showed a great promise to increase classification accuracy in such highly diverse situations. These CNNs first target the phenomena in the image and then classify them (Sharma et al., 2020). Hence, our future work will combine the multipatch method with a multistep image classification CNN.

Once an optimal classification method is developed, aggregation of the multipatch classification results is required. Basing the decision on a single patch result yields a high detection rate but is also more vulnerable to false alarms. On the other hand, only a few patches will be positively classified in the early stages of the disease, and setting a high threshold will result in a high false-negative rate. Hence, setting a policy to aggregate the classification results is crucial to developing an integrated system. In addition to the classification result aggregation, the final decision should also consider other sources of information such as climate conditions, agricultural data including disease prevalence in other plots, crop bread, and previous use of agrochemicals.

Compared to imaging using an airborne camera, this method benefits from the high spatial resolution that enables accurate classification using a low-cost sensor. Today, digital cameras are an accessible technology in cellphones and autonomous vehicles. Thus, short-range imaging can help growers detect crop diseases without the need for sophisticated instrumentation or support from agriculture experts. However, handheld imaging from a short distance lacks the throughput of airborne sensors. Mounting cameras on ground-based, autonomous mobile platforms could improve imaging throughput without sacrificing resolution. Future work will include the research and development of methodologies aimed at real-time optimization of the search path. An adaptive search path that can be modified according to real-time classification results will further increase the scanning throughput. Such an automatic system can provide a high-throughput estimation of the degree of infection in the field. This estimation, combined with environmental parameters (such as humidity, leaf wetness, and temperature), can be used for plants diseases forecasting(Dong et al., 2020). Improving the throughput improves the chances of detecting the disease before it spreads to large areas. Thus, mitigating acts can be taken before significant damage to the crop has occurred.

Funding

This work was supported by the Israel Ministry of Science and Technology Research.

Data availability

Data is available via the following link: Crop Data.

Declaration of Competing Interest

The authors declare that they have no known competing financial interests or personal relationships that could have appeared to influence the work reported in this paper.

References

Adhikari, A., Steffenson, B.J., Smith, K.P., Smith, M., Dill-Macky, R., 2020. Identification of quantitative trait loci for net form net blotch resistance in contemporary barley breeding germplasm from the USA using genome-wide association mapping. Theor. Appl. Genet. 133 (3), 1019–1037. https://doi.org/10.1007/s00122-019-03528-5.

Aharoni, R., Klymiuk, V., Sarusi, B., Young, S., Fahima, T., Fishbain, B., Kendler, S., 2021. Spectral light-reflection data dimensionality reduction for timely detection of yellow rust. Precis. Agric. 22 (1), 267–286. https://doi.org/10.1007/s11119-020-09742-2.

Akino, S., Takemoto, D., Hosaka, K., 2014. Phytophthora infestans: a review of past and current studies on potato late blight. J. Gen. Plant Pathol. 80 (1), 24–37. https://doi.org/10.1007/s10327-013-0495-x.

Arnal Barbedo, J.G., 2019. Plant disease identification from individual lesions and spots using deep learning. Biosyst. Eng. 180, 96–107. https://doi.org/10.1016/j.biosystemseng.2019.02.002.

Atzberger, C., 2013. Advances in remote sensing of agriculture: Context description, existing operational monitoring systems and major information needs. Remote Sens. 5, 949–981. https://doi.org/10.3390/rs5020949.

Ballester, P., Araujo, R.M., 2016. On the performance of googlenet and alexnet applied to sketches, 30th AAAI Conference on Artificial Intelligence, AAAI 2016.

Boulent, J., Foucher, S., Théau, J., St-Charles, P.L., 2019. Convolutional Neural Networks for the Automatic Identification of Plant Diseases. Front. Plant Sci. 10 https://doi.org/10.3389/fpls.2019.00941.

Chan, J.-W., Paelinckx, D., 2008. Evaluation of Random Forest and Adaboost tree-based ensemble classification and spectral band selection for ecotope mapping using airborne hyperspectral imagery. Remote Sens. Environ. 112 (6), 2999–3011. https://doi.org/10.1016/j.rse.2008.02.011.

Dhau, I., Adam, E., Mutanga, O., Ayisi, K., Abdel-Rahman, E.M., Odindi, J., Masocha, M., 2018. Testing the capability of spectral resolution of the new multispectral sensors on detecting the severity of grey leaf spot disease in maize crop. Geocarto Int. 33 (11), 1223–1236. https://doi.org/10.1080/10106049.2017.1343391.

Dong, Y., Xu, F., Liu, L., Du, X., Ren, B., Guo, A., Geng, Y., Ruan, C., Ye, H., Huang, W., Zhu, Y., 2020. Automatic System for Crop Pest and Disease Dynamic Monitoring and Early Forecasting. IEEE J. Sel. Top. Appl. Earth Obs. Remote Sens. 13, 4410–4418. https://doi.org/10.1109/JSTARS.2020.3013340.

Duveiller, G., Defourny, P., 2010. A conceptual framework to define the spatial resolution requirements for agricultural monitoring using remote sensing. Remote Sens. Environ. 114 (11), 2637–2650. https://doi.org/10.1016/j.rse.2010.06.001.

Elshamli, A., Taylor, G.W., Berg, A., Areibi, S., 2017. Domain Adaptation Using Representation Learning for the Classification of Remote Sensing Images. IEEE J. Sel. Top. Appl. Earth Obs. Remote Sens. 10 (9), 4198–4209. https://doi.org/10.1109/JSTARS.2017.2711360.

Feng, Q., Peng, D., Gu, Y., 2019. Research of regularization techniques for SAR target recognition using deep CNN models, in: Yu, H., Pu, Y., Li, C., Pan, Z. (Eds.), Tenth International Conference on Graphics and Image Processing (ICGIP 2018). SPIE, p. 5. https://doi.org/10.1117/12.2524147.

Ferentinos, K.P., 2018. Deep learning models for plant disease detection and diagnosis. Comput. Electron. Agric. 145, 311–318. https://doi.org/10.1016/j.compag.2018.01.009.

Ganin, Y., Ustinova, E., Ajakan, H., Germain, P., Larochelle, H., Laviolette, F., Marchand, M., Lempitsky, V., 2017. In: Domain-Adversarial Training of Neural Networks BT - Domain Adaptation in Computer Vision Applications. Springer International Publishing, Cham, pp. 189–209. https://doi.org/10.1007/978-3-319-58347-1_10.

Giomi, T., Runhaar, P., Runhaar, H., 2018. Reducing agrochemical use for nature conservation by Italian olive farmers: an evaluation of public and private governance strategies. Int. J. Agric. Sustain. 16 (1), 94–105. https://doi.org/10.1080/14735903.2018.1424066.

Hafeez, A.N., Arora, S., Ghosh, S., Gilbert, D., Bowden, R.L., Wulff, B.B.H., 2021. Creation and judicious application of a wheat resistance gene atlas. https://doi.org/10.5281/ZENODO.4469514.

Hedayati, H., McGuinness, B.J., Cree, M.J., Perrone, J.A., 2019. Generalization Approach for CNN-based Object Detection in Unconstrained Outdoor Environments. Int. Conf. Image Vis. Comput. New Zeal. 2019-Decem. https://doi.org/10.1109/IVCNZ48456.2019.8960992.

Hou, L., Samaras, D., Kurc, T.M., Gao, Y., Davis, J.E., Saltz, J.H., 2015. Patch-based Convolutional Neural Network for Whole Slide Tissue Image Classification. Physiol. Behav. 176, 100–106. https://doi.org/10.1016/j.gde.2016.03.011.

Houborg, R., Fisher, J.B., Skidmore, A.K., 2015. Advances in remote sensing of vegetation function and traits. Int. J. Appl. Earth Obs. Geoinf. 43, 1–6. https://doi.org/10.1016/j.jag.2015.06.001.

Hughes, D.P., Salathe, M., 2015. An open access repository of images on plant health to enable the development of mobile disease diagnostics.

J.E. Vanderplank, 2012. Disease Resistance in Plants.

Jayasena, K.W., Van Burgel, A., Tanaka, K., Majewski, J., Loughman, R., 2007. Yield reduction in barley in relation to spot-type net blotch. Australas. Plant Pathol. 36 (5), 429. https://doi.org/10.1071/AP07046.

Kenneth, R., 1960. Aspects of the Taxonomy, Biology and Epidemiology of Pyrenophora Teres Drechsl (Drechslera Teres (Sacc.) Shoemaker), the Causal Agent of Net Blotch Disease of Barley.

Krizhevsky, A., Sutskever, I., Hinton, G.E., 2012. ImageNet Classification with Deep Convolutional Neural Networks. In: Pereira, F., Burges, C.J.C., Bottou, L., Weinberger, K.Q. (Eds.), Advances in Neural Information Processing Systems. Curran Associates Inc.

McIntosh RA, Dubcovsky J, Rogers WJ, Morris C, Appels R, Xia XC, A.B., 2013. Catalogue Of Gene Symbols For Wheat: 2013-2014., in: Proceedings of the 12th International Wheat Genetics Symposium, Yokohama, Japan.

Mohanty, S.P., Hughes, D.P., Salathé, M., 2016. Using deep learning for image-based plant disease detection. Front. Plant Sci. 7, 1–10. https://doi.org/10.3389/fpls.2016.01419.

Mukti, I.Z., Biswas, D., 2019. Transfer Learning Based Plant Diseases Detection Using ResNet50, in. In: 2019 4th International Conference on Electrical Information and Communication Technology (EICT). IEEE, pp. 1–6. https://doi.org/10.1109/EICT48899.2019.9068805.

Murray, G.M., Ellison, P.J., Watson, A., Cullis, B.R., 1994. The relationship between wheat yield and stripe rust as affected by length of epidemic and temperature at the grain development stage of crop growth. Plant Pathol. 43 (2), 397–405. https://doi.org/10.1111/j.1365-3059.1994.tb02701.x.

Pan, S.J., Yang, Q., 2010. A Survey on Transfer Learning. IEEE Trans. Knowl. Data Eng. 22 (10), 1345–1359. https://doi.org/10.1109/TKDE.2009.191.

Qian, N., 1999. On the momentum term in gradient descent learning algorithms. Neural Networks 12 (1), 145–151. https://doi.org/10.1016/S0893-6080(98)00116-6.

Saleem, P., Arif, M., 2019. Plant Disease Detection and Classification by Deep Learning. Plants 8, 468. https://doi.org/10.3390/plants8110468.

Sankaran, S., Mishra, A., Ehsani, R., Davis, C., 2010. A review of advanced techniques for detecting plant diseases. Comput. Electron. Agric. 72 (1), 1–13. https://doi.org/10.1016/j.compag.2010.02.007.

Savary, S., Willocquet, L., Pethybridge, S.J., Esker, P., McRoberts, N., Nelson, A., 2019. The global burden of pathogens and pests on major food crops. Nat. Ecol. Evol. 3 (3), 430–439. https://doi.org/10.1038/s41559-018-0793-y.

Hussain, S., 2020. Computer Vision for Crop Disease [WWW Document]. accessed 2.5.20 Kaggle. https://www.kaggle.com/shadabhussain/cgiar-computer-vision-for-crop-disease.

Sharma, P., Berwal, Y.P.S., Ghai, W., 2020. Performance analysis of deep learning CNN models for disease detection in plants using image segmentation. Information Processing in Agriculture 7 (4), 566–574. https://doi.org/10.1016/j.inpa.2019.11.001.

Shin, Y., Balasingham, I., 2017. Comparison of hand-craft feature based SVM and CNN based deep learning framework for automatic polyp classification. In: Annual International Conference of the IEEE Engineering in Medicine and Biology Society (EMBC). IEEE, pp. 3277–3280. https://doi.org/10.1109/EMBC.2017.8037556.

Shorten, C., Khoshgoftaar, T.M., 2019. A survey on Image Data Augmentation for Deep Learning. J. Big Data 6 (1). https://doi.org/10.1186/s40537-019-0197-0.

Soko, T., Bender, C.M., Prins, R., Pretorius, Z.A., 2018. Yield Loss Associated with Different Levels of Stem Rust Resistance in Bread Wheat. Plant Dis. 102 (12), 2531–2538. https://doi.org/10.1094/PDIS-02-18-0307-RE.

Tassis, L.M., Tozzi de Souza, J.E., Krohling, R.A., 2021. A deep learning approach combining instance and semantic segmentation to identify diseases and pests of coffee leaves from in-field images. Comput. Electron. Agric. 186, 106191. https://doi.org/10.1016/j.compag.2021.106191.

Wang, R., Liu, L., Xie, C., Yang, P., Li, R., Zhou, M., 2021. Agripest: A large-scale domain-specific benchmark dataset for practical agricultural pest detection in the wild. Sensors 21, 1–15. https://doi.org/10.3390/s21051601.

Wu, W., Zheng, J., Li, W., Fu, H., Yuan, S., Yu, L., 2020. Domain adversarial neural network-based oil palm detection using high-resolution satellite images 1139406, 5. https://doi.org/10.1117/12.2557829.

Xiaoling Xia, Cui Xu, Bing Nan, 2017. Inception-v3 for flower classification, in: 2017 2nd International Conference on Image, Vision and Computing (ICIVC). IEEE, pp. 783–787. https://doi.org/10.1109/ICIVC.2017.7984661.

Yardimci, O., Ayyıldız, B.Ç., 2018. Comparison of SVM and CNN classification methods for infrared target recognition, in: Sadjadi, F.A., Mahalanobis, A. (Eds.), Automatic Target Recognition XXVIII. SPIE, p. 5. https://doi.org/10.1117/12.2303504.

Yuan, L., Zhang, H., Zhang, Y., Xing, C., Bao, Z., 2017. Feasibility assessment of multi-spectral satellite sensors in monitoring and discriminating wheat diseases and insects. Optik (Stuttg). 131, 598–608. https://doi.org/10.1016/j.ijleo.2016.11.206.

Zheng, Q., Yang, M., Yang, J., Zhang, Q., Zhang, X., 2018. Improvement of Generalization Ability of Deep CNN via Implicit Regularization in Two-Stage Training Process. IEEE Access 6, 15844–15869. https://doi.org/10.1109/ACCESS.2018.2810849.